Periplasmic Loops of Osmosensory Transporter ProP in *Escherichia coli* Are Sensitive to Osmolality[†]

Doreen E. Culham,[‡] Yaroslava Vernikovska,[§] Natalia Tschowri,[‡,||] Robert A. B. Keates,[‡] Janet M. Wood,[‡] and Joan M. Boggs*[,§,⊥]

Department of Molecular Structure and Function, Research Institute, Hospital for Sick Children, Toronto, ON, Canada M5G 1X8, Department of Laboratory Medicine and Pathobiology, University of Toronto, Toronto, ON, Canada M5G 1L5, and Department of Molecular and Cellular Biology, University of Guelph, Guelph, ON, Canada N1G 2W1

Received August 21, 2008; Revised Manuscript Received September 30, 2008

ABSTRACT: ProP is an osmosensory transporter. The activities of ProP and ProP*, a cysteine-less, His_6-tagged ProP variant, increase with osmotic pressure in cells and proteoliposomes. In proteoliposomes, ProP activity is osmolality-dependent only if the magnitude of the membrane potential ($\Delta\Psi$) exceeds 100 mV. Some amino acid replacements rendered ProP activity osmolality-insensitive [e.g., Y44M in transmembrane segment 1 (TMI); S62C in periplasmic loop 1 (loop P1)], whereas others elevated the osmolality at which ProP activates (e.g., A59C). This suggested that the environments and/or conformations of TMI and loop P1 might be osmolality-dependent. This report correlates structural dynamics of ProP with osmoregulation of its transport activity. Residues in periplasmic loops were replaced with Cys, and changes in their environments were detected by monitoring their reactivities with *N*-ethylmaleimide (NEM). Increasing osmolality markedly increased the NEM reactivity of some Cys residues (e.g., C59, loop P1; C415−C418, loop P6) but not others (e.g., C293, loop P4; C348, loop P5). The NEM reactivity of C62 was insensitive to osmolality, as expected. Substitution Y44M rendered the transport activities of ProP*-A59C and ProP*-Q415C, and the NEM reactivities of the introduced Cys, osmolality-insensitive. Furthermore, osmolality did not affect the reactivity of C59 in cells lacking a protonmotive force, consistent with evidence that $\Delta\Psi$ is required for osmosensing by ProP. These results indicate that the osmotically induced increases in NEM reactivity of C59 and C415 in energized bacteria are due to a conformational change of ProP in response to osmolality. They therefore constitute the first direct evidence of an osmotically induced conformational change associated with osmosensing by a transporter.

Osmoregulatory transporters mediate the uptake of organic molecules denoted osmoprotectants, thereby helping cells to avoid dehydration in high osmotic pressure environments. A member of the major facilitator superfamily (MFS),[1] ProP of *Escherichia coli* catalyzes the accumulation of diverse osmoprotectants, including proline, glycine betaine, and ectoine (*1*). In contrast to transporters that are inhibited by increasing osmotic pressure [e.g., LacY (*2*)], ProP activity increases with an increase in osmotic pressure (or water activity) in cells, in right-side-out membrane vesicles (*3*), and, after purification, in proteoliposomes (*4*). BetP of *Corynebacterium glutamicum* (a member of the betaine-choline-carnitine transporter family) and OpuA of *Lactococcus lactis* (ATP binding cassette transporter family) share this behavior. These systems, denoted osmosensory transporters, serve as paradigms for the study of osmosensing (*5*).

ProP is a H^+-solute symporter powered by the protonmotive force ($\Delta\mu_{H^+}$), which is comprised of a pH gradient (ΔpH, alkaline inside the cell) and a membrane potential ($\Delta\Psi$, negative inside) (*1, 3, 6*). $\Delta\Psi$ also controls osmosensing (*2*). Even if ΔpH is present, ProP is inactive in cells, right-side-out cytoplasmic membrane vesicles, and proteoliposomes lacking $\Delta\Psi$. In proteoliposomes, ProP activity is osmolality-insensitive at low $\Delta\Psi$ (e.g., −100 mV), and it becomes a sigmoid function of osmolality as $\Delta\Psi$ approaches that of actively respiring *E. coli* (−137 mV). Thus, at high $\Delta\Psi$ (e.g., −120 to −137 mV), low osmolality (or high water activity) suppresses ProP activity (*2*).

We would like to correlate the structural dynamics of ProP with osmoregulation of its transport activity. Recently, we created a homology model for ProP (*7*), using the crystal

[†] This work was supported by an operating grant (MOP-68904) awarded to J.M.B. and J.M.W. by the Canadian Institutes for Health Research.

* To whom correspondence should be addressed: Department of Molecular Structure and Function, Hospital for Sick Children, 555 University Ave., Toronto, ON, Canada M5G 1X8. Phone: (416) 813-5919. Fax: (416) 813-5022. E-mail: jmboggs@sickkids.ca.

[‡] University of Guelph.

[§] Hospital for Sick Children.

[||] Current address: Institut für Biologie-Mikrobiologie, Freie Universität Berlin, Königin-Luise-Str. 12-16, 14195 Berlin, Germany.

[⊥] University of Toronto.

[1] Abbreviations: $\Delta\mu_{H^+}$, protonmotive force; ΔpH, transmembrane pH gradient; $\Delta\Psi$, membrane potential; Π/RT, osmolality; $\Pi_{1/2}/RT$, osmolality at which ProP activity is half-maximal; a_0, initial rate of proline uptake via ProP; A_{max}, rate of proline uptake via ProP extrapolated to infinite osmolality; BM, biotin maleimide [(3-maleimidylpropionyl)biocytin]; CCCP, carbonyl cyanide *m*-chlorophenylhydrazone; CPK, Corey, Pauling, and Koltun color scheme; DDM, dodecyl maltoside; DMSO, dimethyl sulfoxide; HRP, horseradish peroxidase; MFS, major facilitator superfamily; MOPS, 4-morpholinopropanesulfonic acid; NEM, *N*-ethylmaleimide; TM, transmembrane.

10.1021/bi801576x CCC: $40.75
Published on Web 12/02/2008

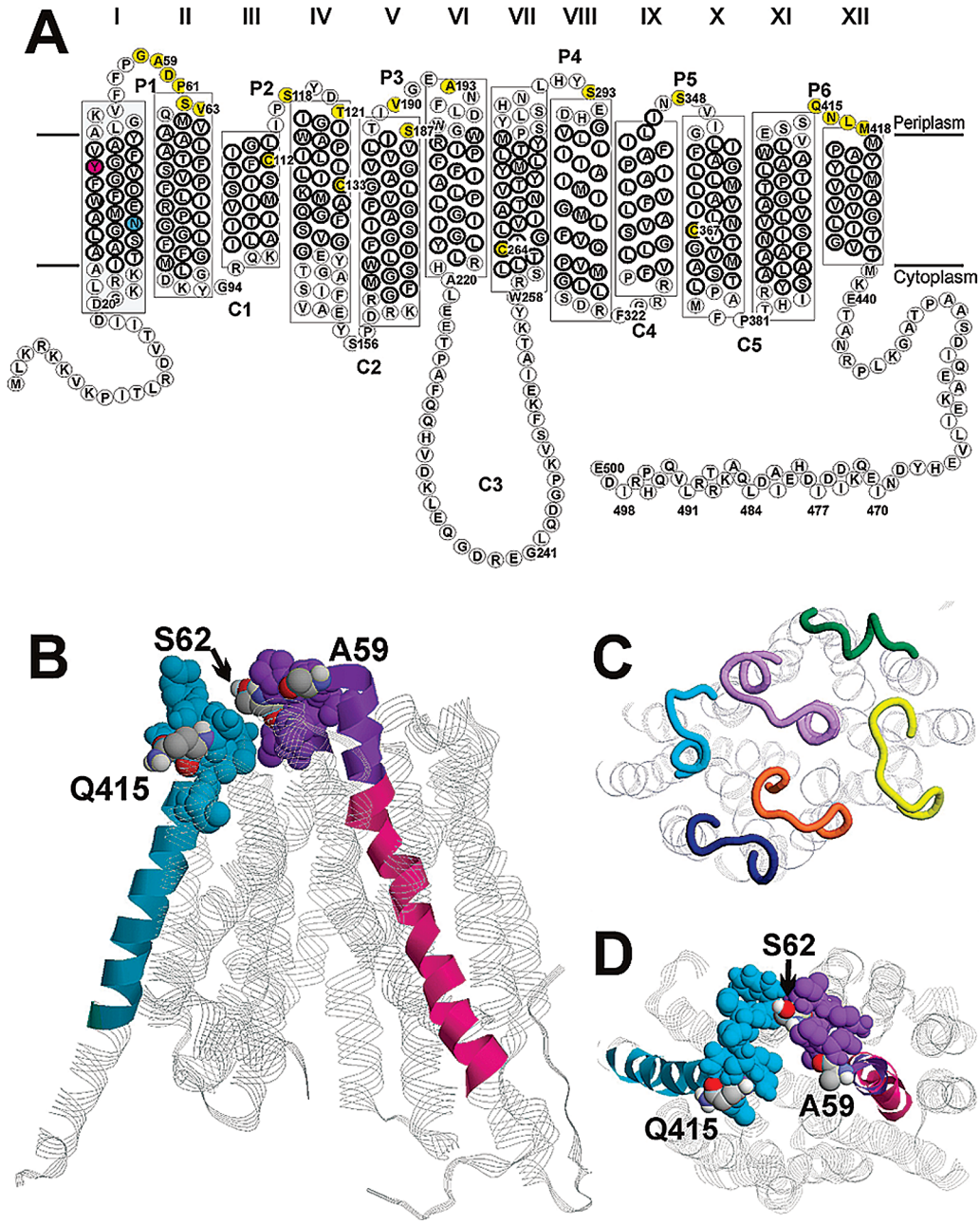

FIGURE 1: (A) Topology of ProP. ProP is predicted to form 12 transmembrane (TM) α-helices linked by 11 hydrophilic loops (periplasmic loops P1−P6 and cytoplasmic loops C1−C5). The illustrated topology is based on a homology model of ProP and substantiated by experimental evidence (*7, 12*). TMI, the subject of this report, is highlighted by a gray box. Native cysteine residues (positions 112, 133, 264, and 367) and residues replaced with cysteines during this study are colored yellow. Residue Y44 is colored magenta and residue N34 turquoise. (B) Location of A59, S62, and Q415 in the ProP model viewed from within the membrane. ProP is in its inward-facing conformation in the model. The ribon portions of TMI and TMXII which are thought to be membrane-spanning are colored pink and turquoise, respectively. Putative loop P6 (residues 409−418) is shown as a turquoise space filling model. Putative loop P1 (residues 50−67) is shown as a purple ribbon on the N-terminal side and a space filling model on the C-terminal side. A59, S62, and Q415 are shown in space filling CPK. TMI tilts toward the center of the structure so that loop P1 would be close to loop P6 in this conformation. (C) Putative periplasmic loops in the ProP model viewed from the periplasm. Loops are shown as strands: P1, residues 50−67 (purple); P2, residues 116−124 (green); P3, residues 188−198 (yellow); P4, residues 286−296 (orange); P5, residues 346−353 (dark blue); and P6, residues 409−418 (turquoise). Loops P2−P6 are around the periphery of the structure, whereas loop P1 extends from the periphery over the center of the structure. (D) Location of several periplasmic residues in the ProP model viewed from the periplasm. P1, P6, TMI, TMXII, A59, S62, and Q415 are indicated as in panel A. S62 is close to residues in P6. The cytosolic loops and cytoplasm-proximal portions of the TMs have been removed from panels C and D for the sake of clarity.

structure of *E. coli* GlpT, an MFS member and glycerol-3-phosphate transporter (*8*), as a template (Figure 1). GlpT shares a common structural topology with other MFS members, including organic anion antiporter OxlT (*9*), H^+-lactose symporter LacY (*10*), and multidrug resistance transporter EmrD (a H^+-solute antiporter) (*11*). The predicted topology and orientation of ProP were substantiated by LacZ−PhoA fusion analysis and fluorescent labeling of cysteine (Cys) residues introduced to the termini, the hydrophilic loops linking putative transmembrane helices (*7*), and TMXII (*12*) of the Cys-less variant ProP* (*13*). In each structure, TMIII, -VI, -IX, and -XII face the surrounding membrane and TMI, -IV, -VII, and -X line a pore to which flanking TM II, -V, -VIII, and -XI also contribute. TMI, -II,

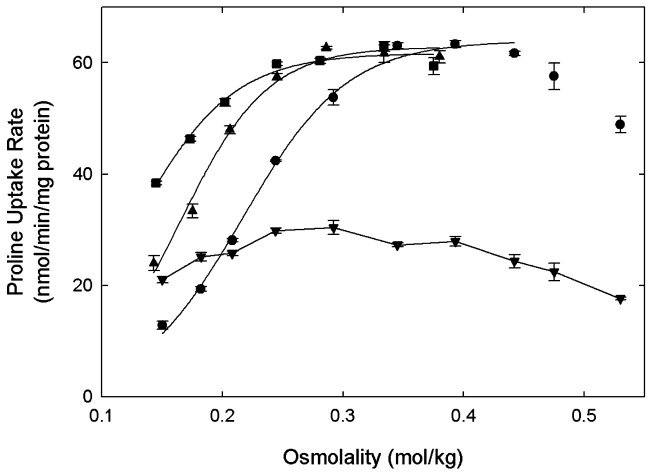

FIGURE 2: Osmosensing by ProP is altered by replacement of residue S62. The variants examined were ProP (●), ProP-S62A (▲), ProP-S62T (■), and ProP-S62C (▼). Variants were created and initial rates of proline uptake measured as described in Experimental Procedures. Data for variants ProP, ProP-S62A, and ProP-S62T were fit to eq 1 (see Experimental Procedures).

and -IV−VI of ProP contain intramembrane ionizable residues that are conserved among ProP homologues and clustered in the N-terminal bundle (*7*). These residues may be directly involved in H^+ or osmoprotectant transport.

The structural dynamics associated with osmosensing by ProP also can be studied by monitoring osmotically induced changes in the reactivity of the introduced Cys residues with alkylating reagents. The impacts of amino acid replacements on ProP function are assessed as they are created. Some replacements render ProP activity quite osmolality-insensitive [e.g., S62C (*7*) and Y44M (described below)]. Others alter the osmolality at which ProP is activated. For example, ProP*-A59C requires a higher osmolality for activation than ProP*. The impacts of these replacements suggest that the environments and/or conformations of transmembrane segment I and loop P1 might be osmolality-dependent.

In this study, we tested this prediction by examining the effect of osmolality on the *N*-ethylmaleimide (NEM) reactivities of Cys residues introduced into periplasmic loops of ProP. Reactive Cys residues of ProP were partially blocked with NEM in intact cells in media of varying osmolality. Cys residues not blocked by NEM were then labeled with biotin maleimide (BM) in membranes under the same conditions for all samples. This procedure revealed those residues whose NEM blockage changed with osmolality in vivo.

Here we report that osmolality increased the rate of reaction of NEM with several periplasmic residues of ProP, with the greatest effect on Cys59. The reaction of NEM with ProP*-S62C and with Y44M variants of ProP*-A59C and -Q415C was osmolality-insensitive, as were their transport activities. Osmolality also did not affect the reaction of NEM with ProP*-A59C in cells lacking $\Delta\mu_{H^+}$, consistent with the fact that the membrane potential ($\Delta\Psi$) is required for osmosensing by ProP. These results indicate that the increase in NEM reactivity of Cys59 and Cys415 in energized bacteria with the increase in osmolality is due to a conformational change of ProP in response to osmolality. It is therefore related to the structural mechanism of osmosensing by ProP.

EXPERIMENTAL PROCEDURES

Materials and Culture Media. Bovine pancreatic DNase I (type II) was from Boehringer-Mannheim (Laval, QC). Egg white lysozyme (UltraPure grade) was obtained from Caledon Laboratories (Georgetown, ON). Oligonucleotides were purchased from Cortec DNA Services (Kingston, ON). Carbonyl cyanide *m*-chlorophenylhydrazone (CCCP), *N*-ethylmaleimide (NEM), ampicillin, β-mercaptoethanol, and imidazole were from Sigma Chemical Co. (St. Louis, MO). Biotin maleimide (BM) [(3-maleimidylpropionyl)biocytin] was from Molecular Probes. Horseradish peroxidase (HRP)-conjugated anti-biotin antibody was from Jackson ImmnoResearch Laboratories, Inc. (West Grove, PA), and HRP-conjugated anti-PentaHis antibody and Ni-NTA resin were from Qiagen, Inc. (Mississauga, ON). Other reagents were of the highest grade available. Solution osmolalities were measured with a Wescor vapor pressure osmometer (Wescor, Logan, UT).

Bacteria were cultivated at 37 °C in LB medium (*14*) or in NaCl-free MOPS media, a variant of the MOPS medium described by Neidhardt et al. (*15*) from which all NaCl had been omitted. This base medium was supplemented with NH_4Cl (9.5 mM) as a nitrogen source and glycerol [0.4% (v/v)] as a carbon source. L-Tryptophan (245 μM) and thiamine hydrochloride (1 μg/mL) were added to meet auxotrophic requirements, creating a complete growth medium with an osmolality of 0.14−0.15 mol/kg. Ampicillin (100 μg/mL) was added as required to maintain plasmids.

Bacteria, Plasmids, and Molecular Biological Manipulations. Basic molecular biological techniques were as described by Sambrook et al. (*16*). Both *proP* expression and ProP activity are osmoregulated (*17*). To focus on the osmoregulation of transporter activity in vivo, genes encoding ProP variants were expressed at a physiological level and in an osmolality-independent manner from the AraC-controlled P_{BAD} promoter (*18*).

ProP variants were expressed in plasmid-bearing derivatives of *E. coli* WG350 [F^- *trp lacZ rpsL thi* Δ(*putPA*)*101* Δ(*proU*)*600* Δ(*proP-melAB*)*212*] (*19*). Each strain contained plasmid pDC79 [a derivative of pBAD24 (*20*) encoding wild-type ProP (*18*)], pDC80 [a derivative of pBAD24 encoding ProP-His_6 (*6*)], pDC117 [a derivative of pBAD24 encoding the fully functional cysteine-less variant of ProP-His_6 with amino acid replacements C112A, C133A, C264V, and C367A, denoted ProP* (*13*)], or a derivative of one of those plasmids. Plasmids encoding these variants were created by site-directed mutagenesis as previously described (*13*).

Structural Modeling. Models were created using Modeler version 9.1 by alignment of the ProP sequence to GlpT [Protein Data Bank (PDB) entry 1PW4] with molecular dynamics refinement set to "very slow" (*21*).

Transport Assays. Published procedures were used to cultivate bacteria in NaCl-free MOPS medium and to measure the rate of proline uptake (*22*). The expression levels of ProP variants were determined by conducting Western blots on whole cell extracts using anti-PentaHis antibodies for ProP-His_6 and ProP* variants or anti-ProP antibodies for ProP variants, as previously described (*18*). The expression levels of the proteins used in this study varied no more than approximately 2-fold (data not shown). Transport assay media were adjusted to the indicated osmolalities with NaCl

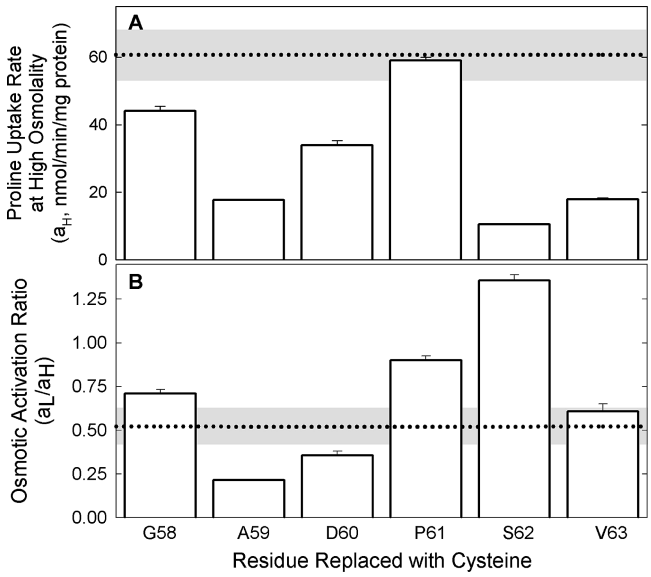

FIGURE 3: Osmosensing is altered by Cys replacement of residues in loop P1. Selected residues in ProP* were replaced with Cys, and initial rates of proline uptake at low (a_L) and high (a_H) osmolalities were determined as described in Experimental Procedures. Horizontal dotted lines and gray boxes represent the mean and standard error of each parameter for ProP-His_6 estimated using cells from 17 separate cultures. (A) Proline uptake activity at high osmolality (a_H). (B) Osmotic activation ratio (a_L/a_H).

or sucrose. For the data reported in Figure 3, initial rates of proline uptake at low and high osmolality (a_L and a_H, respectively) were measured in media supplemented with 50 and 170 mM NaCl to attain osmolalities of 0.24 and 0.49 mol/kg, respectively. All transport measurements were performed in triplicate on at least two separate days. Unless otherwise stated, figures show representative means and standard errors of the mean for triplicate assays performed on one day. The osmotic activation ratio was calculated as a_L/a_H. Where indicated, the initial rate of proline uptake (a_0) attained at a particular medium osmolality (Π/RT) was fit to eq 1:

$$a_0 = A_{max}\{1 + \exp[-(\Pi - \Pi_{1/2})/(RTB)]\}^{-1} \qquad (1)$$

where A_{max} is the uptake rate that would be observed at infinite osmolality, R is the gas constant, T is the temperature, $\Pi_{1/2}/RT$ is the medium osmolality yielding half-maximal activity, and B is a constant inversely proportional to the slope of the response curve.

Site-Directed Alkylation. ProP variants were cultivated in NaCl-free MOPS medium and then reacted with NEM in medium adjusted to different osmolalities with NaCl or sucrose. These conditions were identical to those used for transport assays. NEM stock solutions in ethanol were prepared just before being used. Resuspended cells were added to MOPS media of different osmolalities containing 20 μM NEM and 0.1% ethanol, or a similar amount of ethanol only, and incubated for 20 min at 25 °C. This NEM concentration was found in preliminary experiments to block BM labeling of ProP*-A59C by 50% at low osmolality and was chosen to permit changes in NEM blocking with an increase in osmolality to be detected. After reaction with NEM, cells were washed and frozen at −80 °C for subsequent preparation of membranes as described previously (*13, 23*), labeling of unreacted Cys in membranes with BM, and purification of labeled ProP* variants. BM is accessible to both sides of these membranes (*24*). Samples were not subjected to freeze−thaw cycles because that treatment did not increase the level of BM labeling.

A stock solution of BM was prepared in dimethyl sulfoxide (DMSO), aliquoted, and stored at −20 °C. Membranes were labeled with 0.5 mM BM in 20 mM potassium phosphate (pH 8) (*25*) by incubation for 20 min at room temperature. ProP* variants were purified from membranes on Ni-NTA resin as described previously (*13*) with the following modifications, recommended by Qiagen, Inc., to minimize copurification of other labeled proteins. The cell membranes were solubilized for 30 min at 4 °C, with intermittent vortex mixing, in 100 mM potassium phosphate containing 2 M NaCl, 20% glycerol, 1 mM PMSF, 2 mM β-mercaptoethanol, 20 mM imidazole, and 1% dodecyl maltoside (DDM), adjusted to pH 7.8. The sample was centrifuged at 12000 rpm for 15 min in a microfuge, and the supernatant was added to suspended Ni-NTA resin (50 μL for 25 mL of LB culture), which had been pre-equilibrated with solubilization buffer. The Ni-NTA/supernatant mixture was loaded into a MicroBiospin column, and the column was washed three times with 100 mM potassium phosphate buffer containing 2 M NaCl, 20% glycerol, 1 mM PMSF, 2 mM β-mercaptoethanol, 20 mM imidazole, and 0.04% DDM, adjusted to pH 6.3, and then washed three times with 100 mM potassium phosphate buffer containing 2 M NaCl, 20% glycerol, 1 mM PMSF, 2 mM β-mercaptoethanol, 50 mM imidazole, and 0.04% DDM, adjusted to pH 6.3. ProP* was eluted with 100 mM sodium phosphate buffer containing 20% glycerol, 0.2 M imidazole, 0.04% DDM, and 2 mM β-mercaptoethanol, adjusted to pH 7.4.

Each BM-labeled ProP* variant was analyzed on four 12% Tris-glycine SDS−PAGE gels (Invitrogen, Carlsbad, CA). Protein samples from NEM-treated cells at all osmolalities to be compared and, in some cases from ethanol-treated control cells, were run on the same gel. Two lanes containing two different volumes of each sample were included on each gel. The gels were transferred to nitrocellulose membranes (Bio-Rad Laboratories, Mississauga, ON), and two were used for duplicate Western blots to detect ProP* variants using HRP-anti-PentaHis antibody and an ECL-Plus visualization system as described previously (*13, 18*). Biotin detection was carried out similarly using the other two membranes for duplicate Western blots with HRP-anti-biotin antibody. Since neither antibody could be stripped from the membranes, the density of the band corresponding to BM at the ProP* variant's position on the anti-biotin blot was divided by the density of the band corresponding to the ProP* variant on the anti-PentaHis blot to give the labeling ratio. Any exposed films in which the densities of the paired bands did not increase as expected in proportion to sample loading were discarded. The level of relative BM labeling was obtained by dividing the labeling ratio for cells treated at higher osmolalities by that for cells treated at the lowest osmolality used (~0.15 mol/kg), all run on the same gel. Where labeling at high osmolality is compared to that at low, high is ~0.45 mol/kg. Relative labeling values from duplicate gels were averaged for each experiment.

Labeling of two other unidentified BM-labeled proteins which copurified with ProP* and ran at different positions

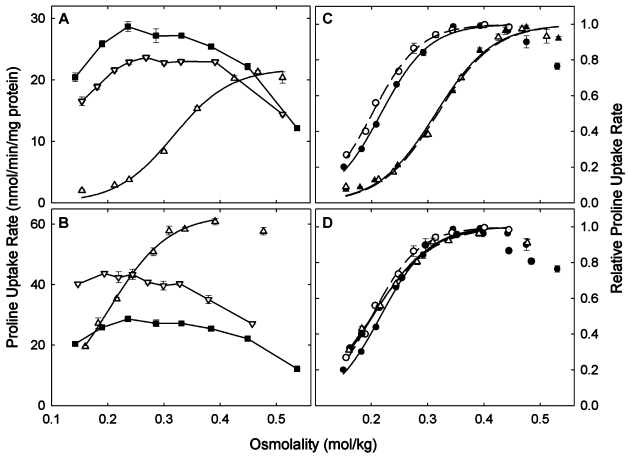

FIGURE 4: Impact of NaCl, sucrose, and mutation Y44M on osmosensing by ProP* variants A59C and Q415C. Variants were created and initial rates of proline uptake measured as described in Experimental Procedures using NaCl (filled symbols) or sucrose (empty symbols) to adjust the transport assay medium osmolality. Initial rates of proline uptake are expressed as absolute uptake rates (A and B) or relative to A_{max} for each variant, determined by regression analysis as described in Experimental Procedures (C and D). Panels A and B show that mutation Y44M has similar effects on the osmotic activation profiles of ProP*, ProP*-A59C, and ProP*-Q415C. Panel A compares the activities of ProP*-A59C (△), ProP*-Y44M (■), and ProP*-Y44M/A59C (▽). Panel B compares the activities of ProP*-Q415C (△), ProP*-Y44M (■), and ProP*-Y44M/Q415C (▽). Note the difference in scale between panels A and B. Panels C and D show that the osmotic activation profiles were independent of the osmolyte used to impose osmotic stress. Panel C compares the activities of ProP (● and ○) and ProP*-A59C (▲ and △). Panel D compares the activities of ProP (● and ○) and ProP*-Q415C (▲ and △). The osmotic activation profiles of ProP* and ProP are also the same (*13*).

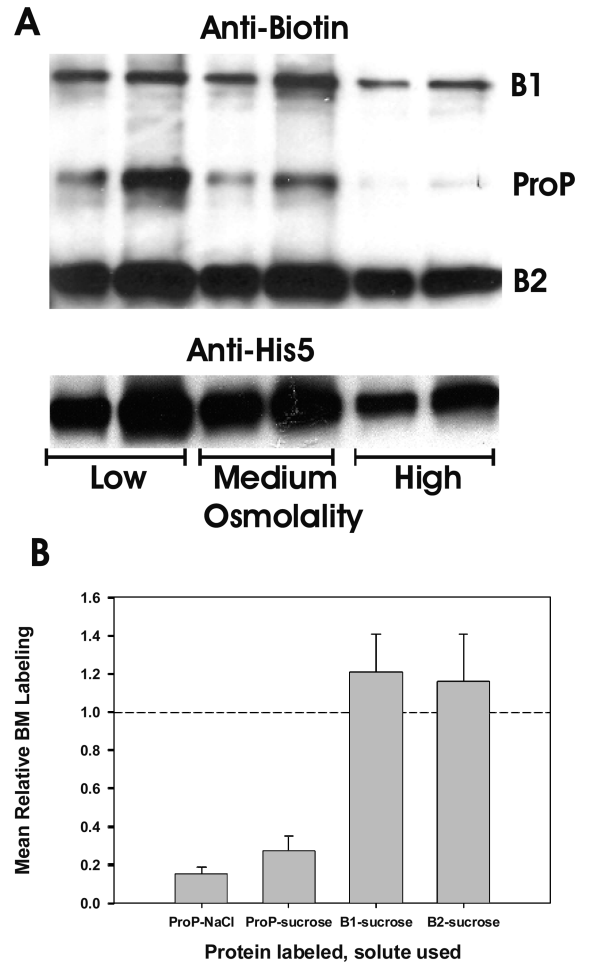

FIGURE 5: BM labeling of ProP*-A59C decreases with an increase in osmolality, indicating an increased level of blocking by NEM. (A) Proteins purified by Ni-NTA chromatography were detected by Western blotting using an anti-biotin antibody (top panel) and anti-PentaHis antibody (bottom panel). Several other biotin-labeled proteins were copurified with ProP. The most prominent, labeled B1 and B2, migrated with apparent M_r values higher and lower than that of ProP, respectively. Two lanes were loaded, one with twice the volume of the other, for cells alkylated with NEM in medium at each osmolality, low (146 mmol/kg), medium (246 mmol/kg), and high (475 mmol/kg) due to addition of sucrose. The labeling ratio was determined as the density of the band on the anti-biotin blot divided by that of the ProP* band on the anti-His blot. (B) BM labeling following NEM blocking of ProP*-A59C or B1 and B2 determined from the labeling ratio at high osmolality relative to that at low osmolality in medium adjusted with NaCl or sucrose. A decrease in the level of BM labeling indicates an increase in the degree of NEM blocking. The dashed line indicates a value of 1.0 for no change in NEM blocking or BM labeling with osmolality. Values represent the means ± the standard deviation of three to six experiments each determined on duplicate gels for each experiment.

on the gel was quantified similarly, if possible, by comparing the BM band densities to that of ProP* on the anti-PentaHis blot, as a measure of protein concentration in the sample. However, the type of gel (percent acrylamide) and the exposure times used for immunoblotting were chosen to optimize transfer of ProP and quantification of anti-biotin band densities for ProP. Sometimes, the higher-molecular mass B1 did not transfer well, or exposure times used for ProP were not optimal for B1 and B2. An example of the former is given in Figure 5A, where the density of B1 did not double with twice as much sample volume loaded. In that case, the data were not used. If the optimally exposed blot for ProP was overexposed for B2, which is also the case in Figure 5A, a less exposed blot was used. Since B1 and B2 are present in every strain used, much more data were obtained for B1 and B2 than for each ProP variant.

To determine how the loss of the membrane potential affected osmolality-dependent labeling of ProP*-A59C, $\Delta\mu_{H^+}$ was dissipated by substituting 10 μM CCCP for glucose in the MOPS medium. A stock solution of 10 mM CCCP was prepared in ethanol. A similar volume of ethanol was added to control cells. Osmolality was varied by adding NaCl.

RESULTS

Refinement of the Structural Model for ProP. The impact of osmolality on the NEM reactivities of introduced cysteines can be interpreted in the context of the structural model for ProP which was recently refined as follows. The published model (PDB entry 1Y8S) was built on an alignment of ProP with GlpT [PDB entry 1PW4 (*7*)]. ProP and GlpT share only 17% identical residues; at this level, simple sequence alignments are as likely to arise by chance as by an actual homologous relationship. To obtain an alignment that was sufficiently reliable for model building, we created multiple-sequence alignments that correlated predicted secondary structure (*26*) and predicted transmembrane segments (*27*) in addition to amino acid sequences. Fine adjustment of the alignment within each TM segment was made by matching residues to the observed statistical preferences among MFS

transporters for contact with the hydrocarbon core of the bilayer and for lateral contacts with adjacent TMs. This gave unambiguous alignments for TMII−TMXII which were consistent with experimental data revealing ProP topology (*7*) and the membrane−aqueous boundaries and environment of residues of TMXII (*12*). For TMI, we were concerned that the alignment might expose N34 to the hydrocarbon region of the bilayer, and for the published model 1Y8S, we chose an alignment that left N34 in contact with the adjacent TMIII.

Subsequently, we have found that N34 can be placed in an outward-facing position of the TMI helix, where it is shielded from the hydrocarbon of the bilayer by neighboring bulky side chains on TMV and -VI, and its side chain contacts the lipid headgroup layer on the cytoplasmic face. A revised model, shown in Figure 1B, was generated with this modification, and a coordinate file in pdb format is provided as Supporting Information. With this modification, the N-terminal end of TMI is shifted up in the bilayer by one residue (Figure 1A), with the result that highly conserved polar residues E37, D40, Y44, R79, K134, Q137, and E144 form a contiguous cluster. Clustering of conserved residues is commonly found in related protein structures, in many cases has been found to indicate a substrate binding site (*28*), and thus provides support for the modification we have made to the original model. This cluster could potentially form a hydrogen-bonded network involved in proton-osmoprotectant symport, as found in other transporters such as ProP homologue LacY (*29*). Substitutions described below are shown in Figure 1A, and their effects on ProP activity and osmolality-dependent reactivities with NEM will be discussed with respect to this model.

Osmotic Activation Profiles of ProP Variants.* The properties of single Cys ProP* variants were explored to identify NEM-reactive transporters with varying functional responses to osmolality. These variants were then used to determine whether changes in ProP structure in response to osmotic stress could be correlated with changes in ProP function. In all cases examined to date, amino acid substitutions have altered the osmotic activation profiles of ProP and ProP* (cysteine-less, His_6-tagged ProP) in the same way (see examples below).

We showed previously that the activities of ProP*-S62C and ProP-S62C are similar and much less osmolality-sensitive than those of ProP* and ProP (*7*). Thus, the structure of loop P1 might change during osmosensing and the osmoregulation of ProP activity. Therefore, the effects of other substitutions for S62 were determined. Substitution of Ala or Thr for S62 had smaller effects on the response to osmolality than substitution S62C. However, all three substitutions elevated the relative activity of ProP at low osmolality (Figure 2). The lower absolute activity of ProP-S62C [like that of ProP*-S62C (*7*)] could reflect a lower turnover number or a lower expression level of this transporter. However, the expression levels of these variants were similar as indicated by Western blotting (data not shown).

In contrast to ProP*-S62C, ProP*-A59C responded to osmolality but required a higher osmolality for activation than ProP (*7*). Therefore, the effects of other Cys substitutions in loop P1 were determined (Figure 3B). The osmotic activation ratio (a_L/a_H) serves as an initial indicator of the impacts of mutations on osmosensing (see Experimental Procedures). It is close to 0.5 for ProP, increases if transporters have relatively high activity at low osmolality (e.g., ProP-S62C, a_L/a_H of approximately 1.2), and decreases if transporters require a high osmolality for activation (e.g., ProP-S59C, a_L/a_H of approximately 0.25) (*13*). This parameter is more robust than absolute transporter activity as it is independent of expression level. The osmotic activation ratios for ProP*-G58C, ProP*-D60C, and ProP*-V63C were similar to that of ProP (Figure 3B). In contrast, ProP*-P61C had an activation ratio close to 1. The activation ratios for ProP* variants with Cys substitutions in other periplasmic loops, S118C, T121C, S187C, V190C, A193C, S293C, Q415C, N416C, L417C, and M418C, were more similar to that of wild-type ProP, suggesting that they were similarly responsive to osmolality (*13, 18*). ProP*-S348C, created to provide a Cys substitution in loop P5, had good activity [a_H of 59.7 ± 0.6 nmol min^{-1} (mg of protein)$^{-1}$] and an a_L/a_H in the wild-type range (0.67 ± 0.01).

While this work was in progress, we found that the activity of variant ProP-Y44M varied little with osmolality and the Y44M replacement could render single-Cys variants of ProP* quite osmolality-insensitive (Figure 4A,B). This allowed us to explore the NEM reactivities of selected Cys residues in the context of osmolality-sensitive and -insensitive ProP* variants (see below).

Impact of Osmolality on the NEM Reactivities of Single-Cys ProP Variants.* Since osmolality had little effect on the activities of ProP*-S62C and ProP*-P61C, it was not expected to induce conformational changes which would alter the NEM reactivities of those Cys residues. However, changes in osmolality might alter the environments of Cys introduced into loop P1 at other positions. The effect of changes in osmolality on NEM reactivity of these Cys was determined. NEM does not have a reporter group, so NEM blocking of Cys was assessed by back-labeling unreacted Cys with BM, which can be detected on a Western blot with an anti-biotin antibody.

Although stringent conditions were used to purify labeled ProP* (*13*; see Experimental Procedures), several other BM-labeled proteins were copurified as shown on the anti-biotin Western blot in Figure 5A. The two primary bands other than ProP are labeled B1 and B2. Only ProP* reacted with anti-His antibody. No other BM-labeled protein was evident at the apparent M_r of ProP* when this procedure was applied to an *E. coli* strain that lacks ProP (WG350 pBAD24, data not shown). An increase in osmolality due to addition of NaCl or sucrose decreased the extent of BM labeling of ProP*-A59C, indicating that it caused an increased level of alkylation of Cys59 by NEM (Figure 5A,B). Varying osmolality did not affect the BM labeling of ProP*-A59C from cells treated with ethanol but not NEM (not shown), indicating that there was no permanent effect of osmolality on ProP*. Bands B1 and B2 were sufficiently resolved that the reactivities of those proteins with BM could also be quantified. Their NEM alkylation and BM labeling did not change with osmolality, so the effect of osmolality was specific to ProP (Figure 5B).

Since changes in salt concentration might affect protein conformation by altering ionic strength and by altering osmolality, subsequent experiments were carried out by using sucrose to change the osmolality of the medium. At the same osmolality, sucrose and NaCl have very similar effects on

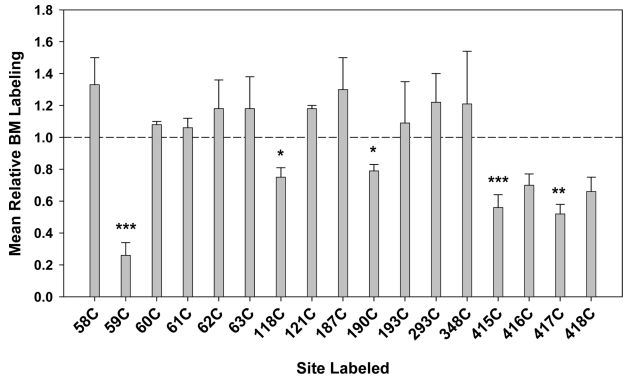

FIGURE 6: Effect of osmolality on BM labeling following NEM blocking of various cysteines in periplasmic loops. BM labeling of Cys substituted at position indicated in ProP* at high osmolality relative to that at low, due to addition of sucrose. A decrease in the level of BM labeling indicates an increase in the level of NEM blocking. The dashed line indicates a value of 1.0 for no change in NEM blocking or BM labeling with osmolality. The values represent the means ± the standard error of three to six experiments for those residues for which statistical analysis was done, and the mean ± range of two experiments for all others. Each was determined on duplicate gels in each experiment. Labeling of residues indicated was significantly different from (weaker than) that of 62C by a Student's *t* test (***$P < 0.001$; **$P < 0.01$; *$P < 0.05$). The only other residue which was labeled in three or more experiments was 58C; its labeling was not significantly different from (stronger than) that of 62C.

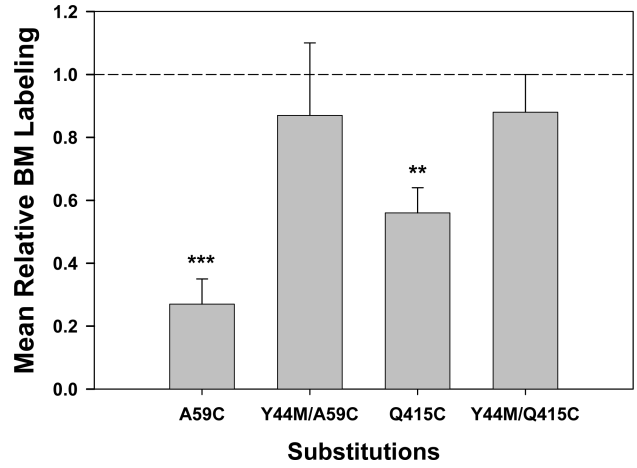

FIGURE 7: Effect of the Y44M substitution in ProP*-A59C and ProP*-Q415C on the responses of Cys59 and -415 to osmolality. BM labeling following NEM blocking at high osmolality relative to that at low osmolality due to addition of sucrose. A decrease in the level of BM labeling indicates an increase in the level of NEM blocking. The dashed line indicates a value of 1.0 for no change in NEM blocking or BM labeling with osmolality. Values represent the means ± the standard error of three to six experiments, each determined on duplicate gels. Labeling of Cys59 and Cys415 in ProP* is significantly different from that in a ProP*-Y44M background [***$P < 0.001$; **$P < 0.01$ (by Student's *t* test)].

the activities of wild-type ProP, ProP*, and other ProP* variants used for this study (this is shown for ProP*, ProP*-A59C, and ProP*-Q415C in Figure 4C,D). They also caused a similar decrease in BM labeling of ProP*-A59C (Figure 5B), whereas they had no effect on labeling of the proteins corresponding to band 1 and band 2 (shown for sucrose in Figure 5B).

The effects of an osmotic upshift on BM labeling of Cys residues located in all the periplasmic loops of ProP are compared in Figure 6. All of these residues (except several in loop P1 and 348 in loop P5, created for this study) were previously shown to react with membrane-impermeant alkylating reagents in cells (*7, 12*). Labeling of ProP*-P61C and ProP*-S62C (loop P1) was not affected by osmolality, as predicted from the unresponsiveness of their activities to osmolality. Of those residues examined, the level of labeling of ProP*-A59C was decreased the most by an osmotic upshift and the decrease was statistically significant. The extent of labeling of ProP*-118C (loop P2) and -190C (loop P3) and of ProP*-415C, -416C, -417C, or -418C (loop P6) decreased by a smaller amount. All of these variants except 416C and 418C were analyzed in triplicate, and their decreased level of labeling was statistically significant (see Figure 6). Increasing osmolality did not increase the level of labeling significantly for any residues examined. The decreased level of BM labeling indicates that these residues were more reactive with NEM at higher osmolality.

When substitution Y44M was introduced into ProP*-A59C or ProP*-Q415C, the effect of osmolality on NEM blocking and BM labeling was greatly reduced (Figure 7), as expected from the decreased effect of osmolality on the activities of these variants (Figure 4A,B). A further correlation between osmolality and the level of labeling of ProP*-A59C is shown in Figure 8A, where the level of BM labeling of ProP*-A59C

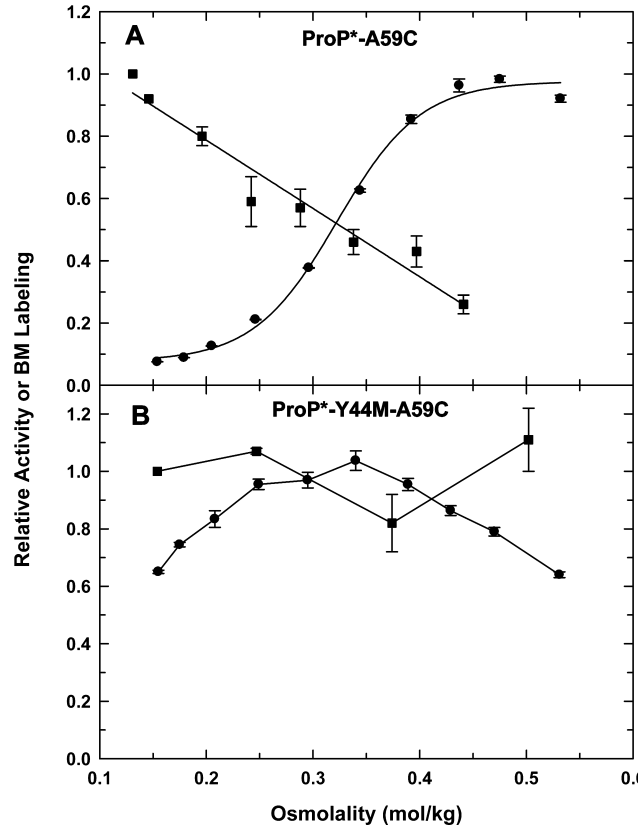

FIGURE 8: Dependence on osmolality of BM labeling and activity of (A) ProP*-A59C and (B) ProP*-Y44M/A59C. BM labeling ratios (■) at each osmolality relative to that at low osmolality and activity relative to A_{max} (●) determined as in Figure 4C,D are shown.

decreases as ProP activity increases with an increase in osmolality. A lack of an effect of osmolality on BM labeling of ProP*-Y44M/A59C parallels the much smaller effect of an increase in osmolality on ProP*-Y44M/A59C activity

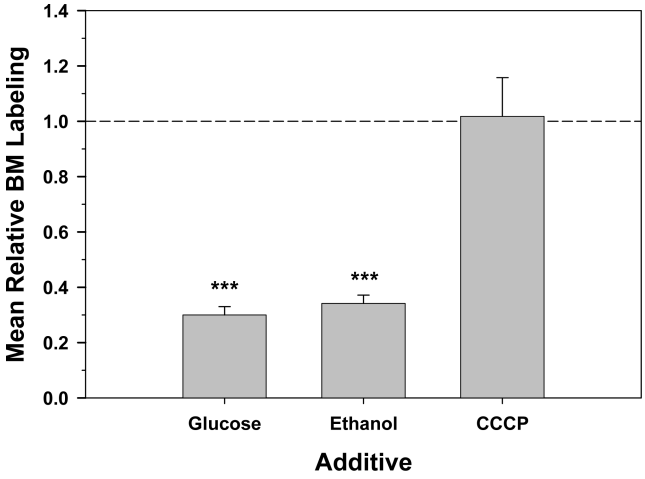

FIGURE 9: BM labeling following NEM blocking of ProP*-A59C in cells with and without a transmembrane potential. BM labeling at high osmolality relative to that at low osmolality due to addition of NaCl in energized cells with a transmembrane potential (presence of glucose), in uncoupled cells lacking a transmembrane potential (presence of CCCP added in ethanol), or in energized cells in the presence of the same volume of ethanol. A decrease in the level of BM labeling indicates an increase in the level of NEM blocking. The dashed line indicates a value of 1.0 for no change in NEM blocking or BM labeling with osmolality. Values represent the means ± the standard error of four samples. Relative labeling of Cys59 in energized cells is significantly different from that in uncoupled cells (***$P < 0.001$ by a Student's t test). The latter are not affected by an osmotic upshift.

(Figure 8B). Thus, the Y44M substitution prevented the osmotic upshift-induced conformational change which resulted in accelerated transport by ProP and an increase in accessibility to NEM of Cys at positions 59 in periplasmic loop P1 and 415 in periplasmic loop P6.

Impact of $\Delta\mu_{H^+}$ on the NEM Reactivity of Cys59. *E. coli* cells respiring in MOPS medium maintain a membrane potential of −140 mV (*30*). The initial rates of proline uptake (nanomoles per minute per milligram of protein) by cells expressing ProP were 92 ± 4 and 0.6 ± 0.5, in transport assay medium containing glucose (the standard medium, osmolality of 0.47 mol/kg) or CCCP (in place of glucose, medium osmolality of 0.46 mol/kg), respectively. The corresponding values for bacteria expressing ProP*-A59C were 33.9 ± 0.4 and 0.6 ± 0.4, respectively. These effects were expected since, as a proton ionophore, CCCP collapses $\Delta\mu_{H^+}$.

To determine whether the absence of $\Delta\mu_{H^+}$ influenced the impact of osmolality on the NEM reactivity of Cys59, NEM blocking was performed in a medium in which CCCP replaced glucose. Osmolality was varied by addition of NaCl to prevent contamination of sucrose with glucose, which could serve as an energy source. Addition of CCCP, but not the ethanol solvent, abolished the effect of high osmolality on BM labeling of A59C as expected (Figure 9). Cys59 was labeled to similar extents at low osmolality in cells that were energized or uncoupled (not shown). This suggests that the environment of this residue is affected by only osmolality in the presence of $\Delta\Psi$.

DISCUSSION

NEM is a small molecule that readily permeates the cell wall and cytoplasmic membrane of *E. coli*. It reacts only with hydrated, ionizable Cys residues (*31*), and therefore, the reactivity of each Cys residue is sensitive to changes in its environment and degree of hydration. Thus, alkylation by NEM is a useful conformational probe for the periplasmic surface of ProP. Reaction of introduced Cys with Cys-specific reagents has been used to delineate static and dynamic features of the structures of a number of proteins, including MFS members lactose permease (LacY) (*32, 33*) and tetracycline/H^+ antiporter [TetA(B)] (*34*). Such studies support the alternating access model for these proteins proposed on the basis of the crystal structures of LacY and GlpT in their inward-facing conformations (*8, 10*) and have shown further that substrate binding to LacY causes opening of a cavity on the periplasmic side and closing of the cavity on the cytoplasmic side (*33, 35*). Generation of a proton electrochemical gradient also increased the reactivity of LacY residues on the periplasmic side in the putative hydrophilic pathway, indicating that it stabilized the outward-facing conformation (*36*).

ProP is powered by the protonmotive force and regulated by the membrane potential ($\Delta\Psi$) and the osmolality (*2*). To investigate the structural mechanism of osmosensing by ProP, we have determined the effect of osmolality on the environments of periplasmic residues. This study shows that an increase in osmolality increased the level of NEM alkylation of cysteines substituted for residues 59 in periplasmic loop P1 and residues 415−418 in periplasmic loop P6 and had smaller effects on cysteines at position 118 in periplasmic loop P2 and position 190 in periplasmic loop P3 as indicated by decreases in subsequent levels of BM labeling of unreacted sites. This indicates an increase in accessibility and/or hydration of these sites with an increase in osmolality. Alkylation of other residues was not significantly affected by an increase in osmolality. A mutation that decreased the dependence of ProP activity on osmolality, Y44M, also greatly reduced the osmolality dependence of the reactivities of Cys59 and Cys415. Although most Cys substitutions did not affect ProP activity or its dependence on osmolality, substitutions P61C (Figure 3) and S62C (*7*) decreased the dependence of ProP activity on osmolality. As expected, the NEM reactivities of these Cys residues were not affected by osmolality, in contrast to that of Cys59. Elimination of $\Delta\mu_{H^+}$ also prevented the effect of osmolality on labeling of ProP*-A59C, as expected from the fact that ProP was active but osmolality-insensitive at low $\Delta\Psi$ (*2*).

These results indicate that the increased accessibility of Cys at positions 59, 118, 190, and 415−418 with an increase in osmolality reflects a conformational response of ProP to osmolality. ProP may respond to osmolality by changing from an inactive conformation to an active conformation, or, as for the effect of $\Delta\mu_{H^+}$ on LacY, it might change from the inward-facing conformation to the outward-facing conformation. Thus, higher osmolality may stabilize ProP in the outward-facing conformation so that it can bind osmoprotectants for transport to the cytoplasm. If this is the case, residues in cytoplasmic loops, particularly those facing toward the center of the hydrophilic cavity, would be expected to be labeled less with an increase in osmolality. Until cytoplasmic hydration is restored by osmoregulatory processes like osmoprotectant uptake via ProP, increasing osmolality increases the degree of cytoplasmic macromolecular crowding and may dehydrate the transporter's cyto-

solic loops. This would facilitate closing of the cavity on the cytosolic side.

Our current model of ProP is shown in Figure 1B with TMI and TMXII highlighted. Because of the tilt of TMI and TMXII, periplasmic loops 1 and 6 approach each other over the periplasmic surface of the structure in this conformation. This is shown more clearly in Figure 1C which looks down on the periplasmic surface of the structure. In all our modeling attempts, with MFS members LacY, EmrD, and GlpT as templates, the TM regions of the transporters are almost superposable, while variable conformations are concentrated in the connecting loops. Thus, the exact structures of the loops are not known, but their positions relative to the overall structure are dictated by the tilt and position of the transmembrane domains. Figure 1C shows that loop P1 extends from the periphery over the central part of the structure, and Figure 1D shows that the C-terminal end of P1 and the N-terminal end of P6 are close together. This proximity may explain why it is residues in loops P1 and P6 that are most affected by osmolality and why several substitutions for S62 affect the activity of ProP. In the outward-facing conformation, loop P1 would have to move away from the center of the structure toward the periphery, which may explain the greater NEM reactivities of Cys at positions 59 and 415−418 at high osmolality.

The membrane potential is also expected to affect the conformation of ProP since ProP is inactive in its absence and becomes osmolality-sensitive when the magnitude of $\Delta\Psi$ exceeds approximately 100 mV (*2*). However, Cys at position 59 was similarly reactive with NEM at low osmolality in the absence of $\Delta\Psi$ and in its presence. Further studies of the effect of $\Delta\Psi$ and of osmolality on the environment of different residues should reveal more insight into the osmolality-sensitive conformation of ProP and the structural mechanism of osmosensing by ProP.

SUPPORTING INFORMATION AVAILABLE

A coordinate file of the revised ProP model shown in Figure 1. This material is available free of charge via the Internet at http://pubs.acs.org.

REFERENCES

1. MacMillan, S. V., Alexander, D. A., Culham, D. E., Kunte, H. J., Marshall, E. V., Rochon, D., and Wood, J. M. (1999) The ion coupling and organic substrate specificities of osmoregulatory transporter ProP in *Escherichia coli*. *Biochim. Biophys. Acta 1420*, 30–44.
2. Culham, D. E., Romantsov, T., and Wood, J. M. (2008) Roles of K^+, H^+, H_2O and $\Delta\Psi$ in solute transport mediated by major facilitator superfamily members ProP and LacY. *Biochemistry 47*, 8176–8185.
3. Milner, J. L., Grothe, S., and Wood, J. M. (1988) Proline porter II is activated by a hyperosmotic shift in both whole cells and membrane vesicles of *Escherichia coli* K12. *J. Biol. Chem. 263*, 14900–14905.
4. Racher, K. I., Voegele, R. T., Marshall, E. V., Culham, D. E., Wood, J. M., Jung, H., Bacon, M., Cairns, M. T., Ferguson, S. M., Liang, W.-J., Henderson, P. J. F., White, G., and Hallett, F. R. (1999) Purification and reconstitution of an osmosensor: Transporter ProP of *Escherichia coli* senses and responds to osmotic shifts. *Biochemistry 38*, 1676–1684.
5. Wood, J. M. (2006) Osmosensing by bacteria. *Science's STKE 357*, pe43.
6. Racher, K. I., Culham, D. E., and Wood, J. M. (2001) Requirements for osmosensing and osmotic activation of transporter ProP from *Escherichia coli*. *Biochemistry 40*, 7324–7333.
7. Wood, J. M., Culham, D. E., Hillar, A., Vernikovska, Ya. I., Liu, F., Boggs, J. M., and Keates, R. A. B. (2005) Structural model for the osmosensor, transporter, and osmoregulator ProP of *Escherichia coli*. *Biochemistry 44*, 5634–5646.
8. Huang, Y., Lemieux, M. J., Song, J., Auer, M., and Wang, D.-N. (2003) Structure and mechanism of the glycerol-3-phosphate transporter from *Escherichia coli*. *Science 301*, 616–620.
9. Hirai, T., Heymann, J. A., Shi, D., Sarkar, R., Maloney, P. C., and Subramaniam, S. (2002) Three-dimensional structure of a bacterial oxalate transporter. *Nat. Struct. Biol. 9*, 597–600.
10. Abramson, J., Smirnova, I., Kasho, V., Verner, G., Kaback, H. R., and Iwata, S. (2003) Structure and mechanism of the lactose permease of *Escherichia coli*. *Science 301*, 610–615.
11. Yin, Y., He, X., Szewczyk, P., Nguyen, T., and Chang, G. (2006) Structure of the Multidrug Transporter EmrD from *Escherichia coli*. *Science 312*, 741–744.
12. Liu, F., Culham, D. E., Vernikovska, Ya. I., Keates, R. A. B., Boggs, J. M., and Wood, J. M. (2007) Structure and function of the XIIth transmembrane segment in osmosensor and osmoprotectant transporter ProP of *Escherichia coli*. *Biochemistry 46*, 5647–5655.
13. Culham, D. E., Hillar, A., Henderson, J., Ly, A., Vernikovska, Ya. I., Racher, K. I., Boggs, J. M., and Wood, J. M. (2003) Creation of a fully functional, cysteine-less variant of osmosensor and proton-osmoprotectant symporter ProP from *Escherichia coli* and its application to assess the transporter's membrane orientation. *Biochemistry 42*, 11815–11823.
14. Miller, J. H. (1972) *Experiments in Molecular Genetics*, Cold Spring Harbor Laboratory Press, Plainview, NY.
15. Neidhardt, F. C., Bloch, P. L., and Smith, D. F. (1974) Culture medium for enterobacteria. *J. Bacteriol. 119*, 736–747.
16. Sambrook, J., Frisch, E. F., and Maniatis, T. (1989) *Molecular Cloning: A Laboratory Manual*, 2nd ed., Cold Spring Harbor Laboratory Press, Plainview, NY.
17. Kempf, B., and Bremer, E. (1998) Uptake and synthesis of compatible solutes as microbial stress responses to high osmolality environments. *Arch. Microbiol. 170*, 319–330.
18. Culham, D. E., Tripet, B., Racher, K. I., Voegele, R. T., Hodges, R. S., and Wood, J. M. (2000) The role of the carboxyl terminal α-helical coiled-coil domain in osmosensing by transporter ProP of *Escherichia coli*. *J. Mol. Recognit. 13*, 1–14.
19. Culham, D. E., Lasby, B., Marangoni, A. G., Milner, J. L., Steer, B. A., van Nues, R. W., and Wood, J. M. (1993) Isolation and sequencing of *Escherichia coli* gene *prop*. *J. Mol. Biol. 229*, 268–276.
20. Guzman, L.-M., Belin, D., Carson, M. J., and Beckwith, J. (1995) Tight regulation, modulation, and high-level expression by vectors containing the arabinose P_{BAD} promoter. *J. Bacteriol. 177*, 4121–4130.
21. Sali, A., and Blundell, T. L. (1993) Comparative protein modelling by satisfaction of spatial restraints. *J. Mol. Biol. 234*, 779–815.
22. Culham, D. E., Henderson, J., Crane, R. A., and Wood, J. M. (2003) Osmosensor ProP of *Escherichia coli* responds to the concentration, chemistry and molecular size of osmolytes in the proteoliposome lumen. *Biochemistry 42*, 410–420.
23. Ye, L., and Maloney, P. C. (2002) Structure/function relationships in OxlT, the oxalate/formate antiporter of *Oxalobacter formigenes*. *J. Biol. Chem. 277*, 20372–20378.
24. Fu, D. X., and Maloney, P. C. (1998) Structure-function relationships in OxlT, the oxalate/formate transporter of *O. formigenes*. *J. Biol. Chem. 273*, 17962–17967.
25. Ye, L., Jia, Z., Jung, T., and Maloney, P. C. (2001) Topology of OxlT, the oxalate transporter of *Oxalobacter formigenes*, determined by site-directed fluorescence labeling. *J. Bacteriol. 183*, 2490–2496.
26. Jones, D. (1999) Protein secondary structure prediction based on position-specific scoring matrices. *J. Mol. Biol. 292*, 195–202.
27. Jones, D. T., Taylor, W. R., and Thornton, J. M. (1994) A model recognition approach to the prediction of all-helical membrane protein structure and topology. *Biochemistry 33*, 3038–3049.
28. Lee, L., Redfern, O., and Orengo, C. (2007) Predicting protein function from sequence and structure. *Nat. Rev. Mol. Cell Biol. 8*, 995–1004.
29. Guan, L., and Kaback, H. R. (2006) Lessons from Lactose Permease. *Annu. Rev. Biophys. Biomol. Struct. 35*, 67–91.
30. Tran, Q. H., and Unden, G. (1998) Changes in the proton potential and the cellular energetics of *Escherichia coli* during growth by aerobic and anaerobic respiration or by fermentation. *Eur. J. Biochem. 251*, 538–543.

31. Karlin, A., and Akabas, M. H. (1998) Substituted-cysteine accessibility method. *Methods Enzymol. 293*, 123–145.
32. Sorgen, P. L., Hu, Y., Guan, L., Kaback, H. R., and Girvin, M. E. (2002) An approach to membrane protein structure without crystals. *Proc. Natl. Acad. Sci. U.S.A. 99*, 14037–14040.
33. Kaback, H. R., Dunten, R., Frillingos, S., Venkatesan, P., Kwaw, I., Zhang, W., and Ermolova, N. (2007) Site-directed alkylation and the alternating access model for LacY. *Proc. Natl. Acad. Sci. U.S.A. 104*, 491–494.
34. Tamura, N., Konishi, S., Iwaki, S., Kimura-Someya, T., Nada, S., and Yamaguchi, A. (2001) Complete cysteine-scanning mutagenesis and site-directed chemical modification of the Tn10-encoded metal-tetracycline/H^+ antiporter. *J. Biol. Chem. 276*, 20330–20339.
35. Zhou, Y., Guan, L., Freites, J. A., and Kaback, H. R. (2008) Opening and closing of the periplasmic gate in lactose permease. *Proc. Natl. Acad. Sci. U.S.A. 105*, 3774–3778.
36. Nie, Y., Ermolova, N., and Kaback, H. R. (2007) Site-directed alkylation of LacY: Effect of the proton electrochemical gradient. *J. Mol. Biol. 374*, 356–364.

BI801576X